Inelastic flow processes in nanometre volumes of solids

1990 J. Phys.: Condens. Matter 2 5317

(http://iopscience.iop.org/0953-8984/2/24/004)

J. Phys.: Condens. Matter **2** (1990) 5317–5326. Printed in the UK

Inelastic flow processes in nanometre volumes of solids

A P Sutton and J B Pethica
Department of Materials, Oxford University, Parks Road, Oxford OX1 3PH, UK

Received 29 January 1990

Abstract. We consider the types of inelastic process that may occur in very small volumes of material, using the model system of a sharp tip coming into contact with a flat. Both molecular dynamics simulations and experimental results are presented. Theoretical lattice strength is observed, adhesion between clean surfaces is strong and involves inelastic flow, and the adhesion is considerably reduced by differing atomic species at the interface. The MD simulations, using long-range potentials, show that the processes likely to be occurring include local sintering or diffusion-like flow, enhanced by local soft modes, and net material transfer upon adhesive unloading.

1. Introduction

In this paper we consider, via both theoretical modelling and experimental evidence, the nature of mechanically induced irreversible or inelastic flow in very small volumes of solids. Although it might appear to be of interest only for novel nanometre or thin film structures, in fact this question of the onset of plastic flow in small volumes also underlies the macroscopic processes of adhesion, friction and fracture, because the properties of very small asperities or crack tip regions often control the macroscopic behaviour.

We note that in nanometre volumes, many normal macroscopic flow processes may not take place; for example there may happen to be no dislocations or sources present within the stressed volume. To this we must also add the wide range of surface effects in crystal plasticity, where atomic scale surface chemistry can dramatically influence bulk crystal deformation. A considerable number of these Rehbinder effects are unexplained [1]. Since nanometre volumes have a high surface-to-volume ratio, they provide an excellent means for investigating these surface effects. We might even expect that effects on plasticity in nanometre volumes are the means by which surface composition influences bulk deformation. Surface chemical effects in the onset of plasticity require atomistic rather than continuum analysis, because a single monolayer of impurities is unlikely to have a significant effect on the elastic response of the system. Flow in 'nanovolumes' also addresses the wider question of defect nucleation, which is controlled by relatively small numbers of atoms. Standard theories, for example of dislocation nucleation [2], are based on continuum theory and they provide an inadequate description of the discrete atomic and non-linear processes involved. Their usefulness is thus limited, particularly in view of their critical dependence on values of local parameters such as surface energy due to a single atomic step.

Atomistic simulations of crack propagation have been made [3], but they are invariably two-dimensional in nature and therefore difficult to relate to experiments.

0953-8984/90/245317 + 10 $03.50

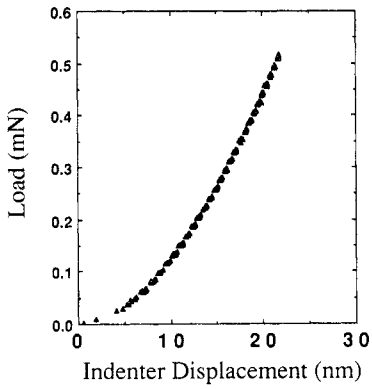

Figure 1. The displacement of the diamond tip normal to the electropolished tungsten surface as a function of applied loading—below the critical value. From [5].

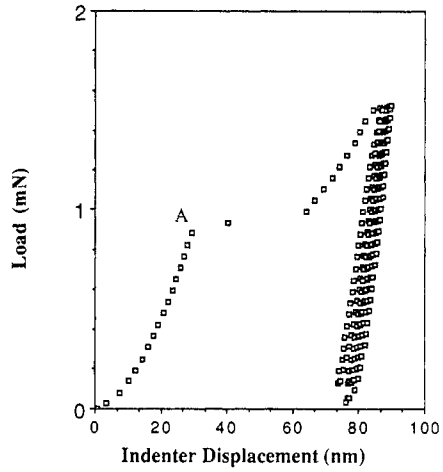

Figure 2. The displacement of the diamond tip normal to electropolished tungsten surface as a function of applied loading—above the critical value. From [5].

Here we use the tip–flat geometry as in the scanning tunnelling and atomic force microscopes, which given an experimentally realisable 3D system, yet has a small enough number of atoms to allow full molecular dynamics simulations. We have treated aspects of the approach to contact elsewhere [4]; in this paper we focus mainly on the processes once in contact. The forces and displacements due to tip surface interactions can now be measured directly. Also the geometry allows good control, in UHV, of the surface atomic composition. The experiments show that theoretical lattice strength can be observed for low defect density surfaces, and that clean surfaces can show significant, load-independent adhesion. MD simulations, using long-range potentials, show the processes likely to be occurring. Sintering is seen along with net material transfer upon adhesive unloading. Both are good examples of the aid to interpretation of experimental data brought by simulation, in that neither process had been clearly identifiable in the data.

2. Experimental details

Two types of experiment have been performed using the tip–flat geometry. The first involves the use of a sharp diamond tip contacting a flat, the displacement of the tip being measured with sub-Ångström resolution as a function of the force applied to the tip. Details of the experimental method are given elsewhere [5]. The essential feature of the method is that the contact area can be determined from the compliance, since the elastic modulus is known. Furthermore, any hysteresis in the flow in the contact is clearly observable, and the sensitivity is such that single-atom displacements are in principle observable. A variety of contact properties have been studied with this apparatus but we focus here on one particular result, shown in figure 1. The curve shows the result of applying a load to an electropolished tungsten surface, and it depicts the data from four complete cycles of loading up and back down again. It is seen that the displacements are almost perfectly reversible, that is, no inelastic flow has occurred in the contact. In contrast, if the load is taken above a critical value (around 1 mN), the behaviour is as in

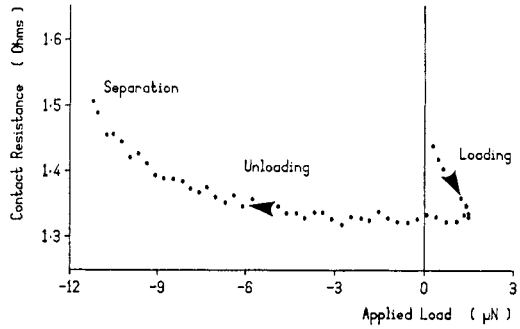

Figure 3. The variation of the contact resistance between the tungsten tip and nickel flat as a function of normal load–light loading conditions. From [6].

figure 2. Once the critical value is reached (point A) the tip moves abruptly into the surface, and subsequent unloading shows a substantial hysteresis; extensive plastic flow suddenly occurs. Even subsequent load–unload cycles, as depicted, show detectable Bauschinger-like hysteresis. The striking feature of these data is that we can calculate the stress at the surface at A from standard Hertz analysis, knowing only the elastic moduli of the tungsten and diamond. From this we find that the shear strain just beneath the surface reaches 8%. Clearly, in the sub-micrometre volume under the tip, something very close to the theoretical lattice strength is attainable. If the tungsten surface is mechanically rather than electropolished, such high strengths are not seen, although the shear strains are still considerably in excess of normal macroscopic values. This suggests that essentially defect-free regions are required to observe the theoretical strength; by implication surface steps etc, which must also be present on the electropolished surfaces, are not able to nucleate significant plastic flow. More details are given elsewhere [5]. The important experimental aspects are that the contact stress and hence shear strain can be directly calculated, and that the stressed volume is sufficiently small (at 100–200 nm across) that no low-stress dislocation sources will be present or operable for the electropolished surface.

Since the above experiment is performed in air it is not suitable for quantitative observation of adhesion or phenomena occurring upon unloading, where stresses immediately at the interface are important. To achieve atomically clean and controlled surfaces, experiments have been performed in an ultra-high-vacuum system, with ion beam cleaning and Auger spectroscopy facilities. The surfaces were routinely cleaned to impurity levels of 1% of a monolayer. Details have been described elsewhere [6]. These experiments were performed before the development of the tip displacement sensing method described earlier; instead, assessment of contact area was made by recording the resistance of the contact. When the surfaces are clean, this gives a reasonable estimate of area from the Maxwell or Sharvin constriction resistance formulae, and more importantly allows observation of any hysteresis in the load–unload cycle. However, when monolayer films are present on the surface it is not able to give accurate quantitative estimates of contact stress. Figure 3 shows the behaviour of contact resistance with load for a clean tungsten tip and nickel flat. There is substantial hysteresis (of contact area) implying some kind of inelasticity, and for a significant part of the unloading, the contact area is roughly constant. The adhesion, or final pull-off force for such small initial loads is in fact nearly independent of the initial applied load [6]. At higher loads, the adhesion force becomes proportional to the applied load. These results can be understood qualitatively if the surface forces act as an additional applied load, and if the adhesional separation process is in some sense ductile, and hence the adhesion force proportional to contact area. Adhesion at low loads is also affected by monolayer

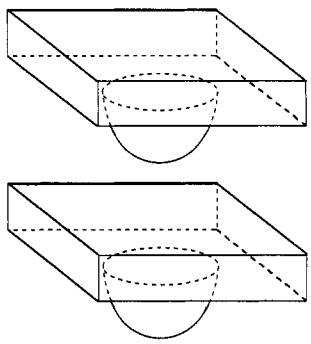

Figure 4. A schematic outline of the simulation cell envelope, showing two cells.

concentrations of adsorbates [6]. Finally, calculating the contact area from the resistance suggests that in these experiments also, shear strains several times the macroscopic bulk values of the metals are present in the contact. Due to the uncertainties in conductivity mentioned above we cannot say from these data whether a monolayer of oxide affects the flow stress, which is of particular interest on unloading.

We may summarise the above results as follows. Firstly, stresses approaching the theoretical lattice limit may be present in these very small contacts; secondly, adhesion between clean surfaces is strong, and involves inelastic flow; thirdly, the adhesion is considerably reduced by differing atomic species at the interface. From this it is clear that high strain inelasticity is present, but the actual processes of relief of this stress are not clear. In particular we do not know if the inelastic flow involves local diffusion, dislocation motion, or homogeneous shear of two whole layers of atoms ('block slip'), for which there is other microcontact evidence [7]. We do not know how nucleation events are controlled, although they are clearly affected by the interfacial chemistry. In particular for friction and wear, it is important to know if material transfer occurs in the contact; we attempted to show this using sub-micrometre Auger in the above apparatus, but the experiments are extremely difficult and rather inconclusive. To cast some light on these mechanisms of local inelasticity, we have set up an atomistic simulation of the tip approach–pull-off process of a broadly similar tip and flat surface arrangement.

3. Molecular dynamics simulations

Molecular dynamics simulations of a tip interacting with a surface have been performed using a Lennard-Jones 6–12 potential. The geometry of the simulation cell is shown schematically in figure 4. Periodic boundary conditions were applied in all three directions. The normal to the substrate was (001) and the tip had the same orientation and FCC crystal structure as the substrate. The substrate slab had dimensions $11a$ by $11a$ by $3a$ (a is the FCC lattice parameter) and it contained 1694 atoms. The tip was constructed by selecting atoms in an FCC crystal falling within a paraboloid with a radius of curvature of $1a$ and a height of $5a$. The tip contained 273 atoms, giving 1967 atoms in total. As shown in figure 4 the tip was attached to the underside of the substrate. By varying the length of the computational cell in the z direction it was possible to control the height of the tip above the substrate in the periodic image cell below. Thus the tip is also interacting with the top surface of each slab through the periodic boundary conditions. Using this geometry all atoms were treated dynamically and the equations of motion were integrated with the velocity Verlet algorithm [8]. The potential was cut off at $2a$, leading

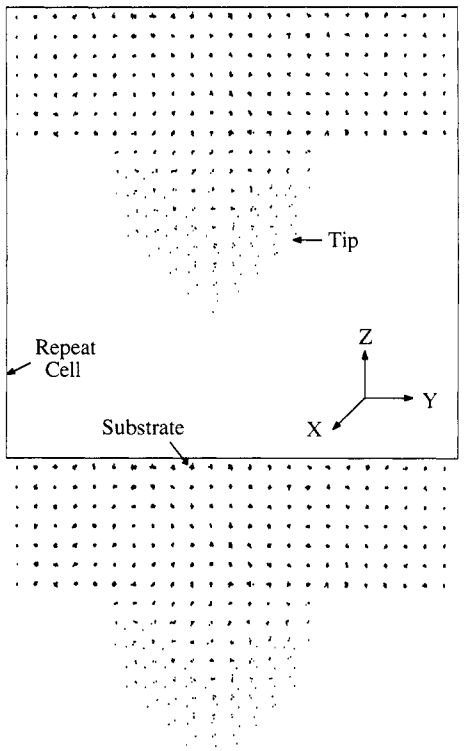

Figure 5. A snap-shot of the tip and substrate after initial equilibriation of 2000 time steps. Two repeat cells along the z axis are shown. Note the reconstruction of the tip. There is still no interaction between successive repeat cells along z.

to 140 interacting neighbours in the perfect FCC crystal. In Lennard-Jones reduced units (see [8], p 327) the temperature of the simulation was 0.2 and the time step was 0.01, which corresponds, for solid argon, to a temperature of 20 K and a time step of 40 fs. We estimate, using the data of [9], that the thermodynamic melting point of FCC 'Lennard–Jonesium' is 0.7 in reduced units. Thus our simulation temperature is approximately 0.3 of the bulk melting point. The temperature was maintained constant throughout the run by scaling all particle velocities every time step.

An equilibration run was performed for 2000 time steps. During this run the cell z length was sufficiently large that there were no interactions between adjacent cells in this direction. The thermal expansion in the x and y directions was 2.8%. After this equilibration run no further changes in the cell x and y lengths were allowed. Not surprisingly the tip underwent the largest changes during the equilibrations, as seen in figure 5. The tip was then brought within range of the substrate, initially in discrete jumps followed by re-equilibration runs, and then at a constant strain rate. The strain rate was such that the cell length decreased by $1a$ over 5000 time steps. The strain was applied homogeneously to all atoms in the cell every tenth time step. This was continued until the force of attraction between the tip and the substrate almost reached zero. The tip was then pulled off the substrate by reversing the sense of the strain but keeping its rate constant. This was continued until the tip broke free of the substrate. Changes in the structure of the tip were recorded as snap-shots.

As the tip came within range of the substrate, atoms at the tip base strained increasingly towards the substrate. At the same time those tip atoms underwent larger amplitudes of vibration, with correspondingly lower frequencies. Eventually, when the lowermost tip atom was approximately $1a$ from the substrate on average, it jumped

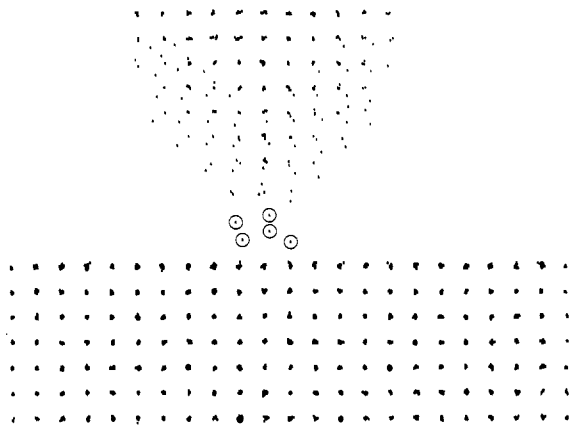

Figure 6. Encircled atoms are undergoing large-amplitude, low-frequency vibrations between the tip and substrate.

across the gap onto the substrate. It then underwent low-frequency oscillations between the tip and the substrate, with rest times on both the tip and the substrate. Continuing the run at a fixed cell length, more atoms at the base of the tip became quasi-detached and underwent these large-amplitude, low-frequency oscillations between the tip and the substrate. Figure 6 shows a snap-shot in which five atoms are undergoing these oscillations. We believe that we are seeing here the initial stages of sintering between the tip and the substrate. It is remarkable that the sintering is occurring not so much by surface diffusion as by greatly enhanced vibrations of the least coordinated atoms in two attractive potential wells that are separated by a barrier, the height of which is comparable to kT. After 10 000 time steps at this fixed cell z length the tip was brought closer to the substrate at the constant homogeneous strain rate. The area of contact increased and a (001) stacking fault was produced at the base of the tip because the total number of tip and substrate (002) planes was 15 and was therefore odd. The fault produced bending and rotation of planes in the tip (which can be seen to the left of C in figure 7). A defect was nucleated at one end of the fault and after a further 2000 time steps both the defect and the fault had vanished and the total number of (002) planes had been reduced to 14. The tip was then in perfect epitaxial contact with the substrate and the force of attraction between the tip and the substrate had reduced to zero. A Burgers circuit analysis revealed that the defect was a $\frac{1}{2}[100]$ dislocation. The dislocation moved by glide and climb diagonally through the tip and emerged from the top left-hand corner of the tip in figure 7. The dislocation is seen in figure 7 approximately midway along its path; the fault to the right of the dislocation has been eliminated by the motion of the dislocation to C.

Although the strain to pull the tip off the substrate was applied homogeneously it became localised at the base of the tip very rapidly. The lowermost three to four planes of the tip became increasingly diffuse and widely spaced, as shown in figure 8. Atoms in these layers performed low-frequency, large-amplitude vibrations normal to the surface of the substrate. On further straining, these layers merged into each other and reformed to produce a new layer, apparently homogeneously, at the tip base. A snap-shot, taken soon after the formation of this new layer, is shown in figure 9. It is seen that the layers are now less diffuse, presumably because their spacing is reduced. On further straining a neck started to appear above the second layer of the tip base. Eventually the tip broke free, leaving a considerable number of tip atoms on the surface of the substrate, as shown in figure 10.

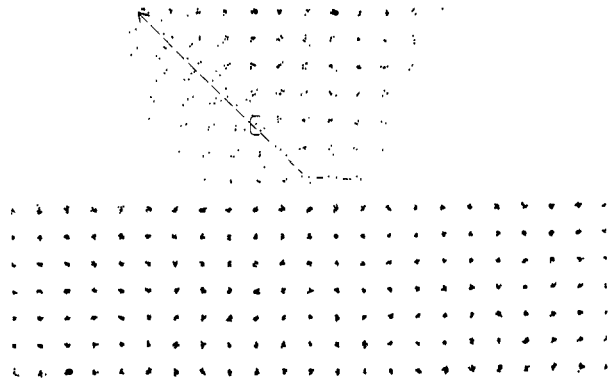

Figure 7. A $\frac{1}{2}[100]$ edge dislocation moving by glide and climb along the path shown. On the left of the dislocation there is a (001) stacking fault between the tip and the substrate. The dislocation centre is at C and the extra half-plane can be seen by viewing along the vertical planes of the figure.

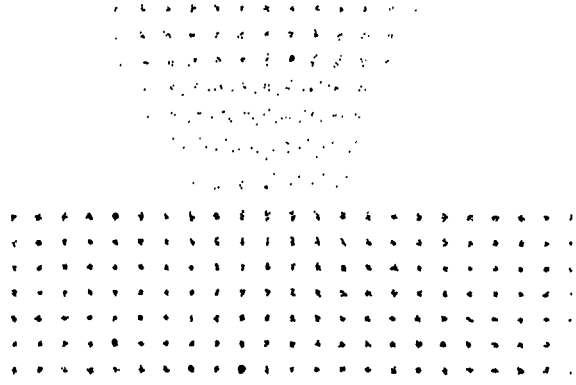

Figure 8. A snap-shot taken just prior to the planar dissociation seen in figure 9. Note the strain localisation at the bottom three layers of the tip, and the diffuseness of those layers.

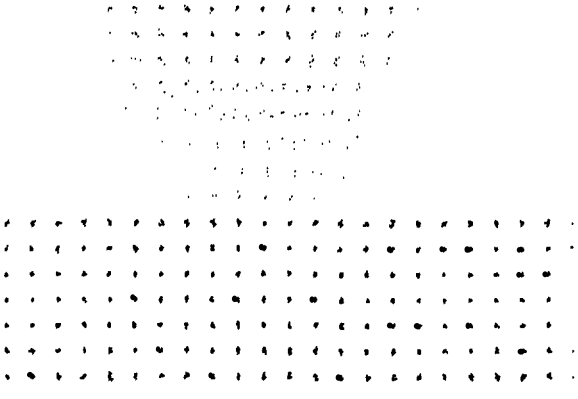

Figure 9. A snap-shot taken just after the planar dissociation at the tip base. Note that there are now eight layers in the tip compared with seven in figure 8. Note also that the layers at the tip are less diffuse than in figure 8.

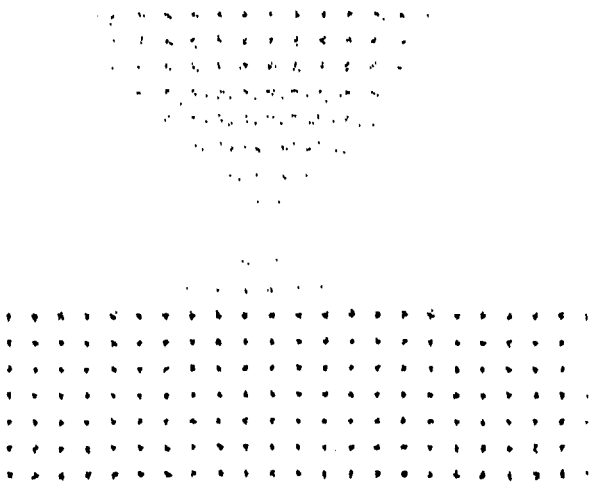

Figure 10. A snap-shot taken after the tip has broken free of the substrate. Note the pile of atoms left on the substrate.

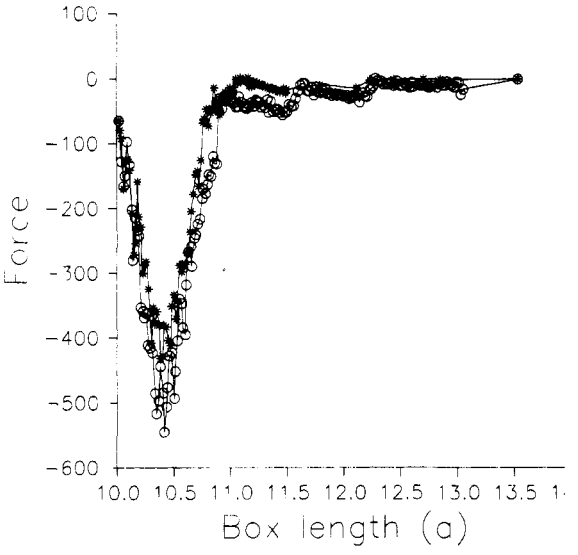

Figure 11. The force separation curve for the entire tip approach–removal cycle. Points represented by stars correspond to the approach sequence and those represented by circles correspond to the removal sequence. All points represent an average calculated over 80 MD time steps. At a box length of $10a$ the tip was in epitaxial contact with the substrate and the sequence was reversed from approach to removal. Note the slightly deeper and wider minimum of the removal sequence. See the text.

Figure 11 shows the force separation relations for the complete approach and separation cycle. The approach sequence is represented by stars and the separation sequence by circles. The force is in Lennard-Jones reduced units and the 'box length' is the length of the computational cell normal to the substrate surface. The box length of $10a$ corresponds to the point at which the sequence was reversed from approach to separation. The deeper and wider minimum of the separation sequence (circles) is evidence of the irreversibility of the whole cycle. However, the hysteresis appears to be much smaller than that seen in figure 3, although in figure 3 the vertical axis is the contact

resistance rather than the force of adhesion. It can be seen that the system is always in tension; we plan to extend the simulation to compression.

4. Discussion and conclusions

Several of the experimental phenomena are shown well in the above simulation, along with a number of less experimentally obvious processes. The presence of very large lattice strains is clearly seen in figures 6 and 7; these reached 12%, which may be compared with the 8% shear deduced from figure 2. Interestingly, the dislocation seen in figure 7 relieved a stress that extended over the entire tip. By contrast, stresses localised to a few atoms between the tip and the surface gave rise to local soft modes and diffusional displacements. This helps to explain why theoretical strengths are experimentally observable despite surface irregularities: local surface defects such as steps, which must be present, may not give rise to extended defects but the stresses to which they give rise may be relieved by diffusional displacements. It is thus likely that differing atomic species at the surface will change the ease of strain accommodation at the interface. An interesting point arising from the simulations is the possible importance of local soft phonon modes—we are not aware that these have been considered before now to contribute to inelastic flow. We note also that true single-atom contacts seem unlikely to be stable, and hence may not be a good system for studying 'quantisation' of resistance [10].

The overall irreversibility of the load–unload process in figure 3 is very evident in the simulation, especially the way in which the contact area remains roughly constant during most of the tensile unloading. At present the simulations are with controlled strain whereas the experiments are with controlled stress, which is why the final necking down under tension, with accompanying reduction of attractive force in the simulations, is not seen in the experiments. This matter has been discussed in continuum systems by Maugis [11]. The process of growth of the contact area resembles sintering and implies that temperature may have an important effect on the experiments; this was not allowed for in earlier analysis of the results [6]. Also, although a dislocation movement was seen in the MD simulations, the tensile failure of the contact did not involve dislocations, despite being clearly inelastic. The data of figure 2 suggest a roughly constant strain for failure (adhesional force proportional to load and contact area). This is a striking demonstration of the importance of a diffusion-like flow at this scale. We can see that the effect of adsorbed oxide on adhesion may be via local diffusion inhibition, and the adhesion determined by the final size of the sintered 'neck' of contact. This implies a time and temperature dependence that ought to be investigated experimentally. The possibility of a diffusion contribution to plastic flow in small indents has also been considered from a continuum point of view by Oliver and Pharr [12], although with very high strains present it is difficult to ascertain suitable values of diffusion constants.

The transfer of material from tip to flat, suspected from the experiments, is clearly seen in the simulations. We may even conjecture that material transfer will always occur when there is a local geometric asymmetry between the contacting bodies, and that the line of failure will start from the edge atoms with lowest coordination number. Again this will be strongly modified by local chemical composition. Introduction of lateral shear into the simulation will provide an interesting view of sliding transfer and junction growth, essential mechanisms in friction [13]. A particularly curious form of material transfer is the jumping across of the tip atom to the surface during the initial approach.

This occurs because of thermal excitation from the low-coordination site at the tip to a more strongly bound position on the flat surface. The process is strikingly similar to the spontaneous tip modification that sometimes occurs in STM imaging, and may contribute to atomic 'writing' which has been shown to be possible with an STM tip [14].

The extent to which simulation and experiment give mutual insights in this important model system is very striking. We expect further understanding of nanometre mechanics and stability to come from experiments involving control and variation of both temperature and strain, and from simulations with adsorbed species at the surfaces and with potentials having both long- and short-range accuracy [15].

It has recently come to our attention that Landman *et al* [16] are performing related simulations and experiments. The main ddifference in the simulations, apart from the choice of interatomic potentials, appears to be the much blunter tip used in [16]. During the approach, Landman *et al* found the same kind of mechanical instability that we observed between two flats in [4], involving the whole tip jumping onto the substrate. By contrast, the instability we have reported here for a much sharper tip is qualitatively different and involves, at least initially, a single atom jumping between the tip and the substrate. We believe this is the reason for a larger force separation hysteresis than in the present work being seen in [16].

Acknowledgments

We are grateful to Uzi Landman and co-workers for a preprint of [16]. APS gratefully acknowledges the support of the Royal Society.

References

[1] Latanision R M and Fourie J T (ed) 1977 *Surface Effects in Crystal Plasticity* (Leyden: Noordhoff)
[2] Rice J R and Thompson R M 1974 *Phil. Mag.* **29** 73
[3] Baskes M I, Foiles S and Daw M 1988 *J. Physique Coll.* **49** C5 483
[4] Pethica J B and Sutton A P 1988 *J. Vac. Sci. Technol.* A **6** 2490
[5] Pethica J B and Oliver W C 1989 *Mater. Res. Symp. Proc.* **130** 13
[6] Pashley M D, Pethica J B and Tabor D 1984 *Wear* **100** 7
[7] Todd J D and Pethica J B 1989 *J. Phys.: Condens. Matter* **1** 9823
[8] Allen M P and Tildesley D J 1987 *Computer Simulation of Liquids* (Oxford: Clarendon)
[9] Hansen J-P and Verlet L 1969 *Phys. Rev.* B **184** 151
[10] Gimzewski J and Möller R 1987 *Phys. Rev.* B **36** 1284
[11] Maugis D 1977 *Le Vide* **186** 1
[12] Oliver W C and Pharr G 1989 *J. Mater. Res.* **4** 94
[13] Bowden F P and Tabor D 1964 *The Friction and Lubrication of Solids* vol 2 (Oxford: Clarendon)
[14] Becker R S, Golovchenko J and Schwarzentruber B S 1987 *Nature* **325** 419
[15] Sutton A P and Chen J 1990 *Phil. Mag. Lett.* **61** 139
[16] Landman U, Luedtke W D, Burnham N A and Colton R J 1990 *Science* at press